Multivariable H(infinity) tracking control of a mono-cycle

MULTIVARIABLE H_∞ TRACKING CONTROL OF A MONO-CYCLE

Bram de Jager, Frans Veldpaus

Faculty of Mechanical Engineering, Eindhoven University of Technology
P.O. Box 513, 5600 MB Eindhoven, The Netherlands
Fax: +31 40 2461418 Email: A.G.de.Jager@wfw.wtb.tue.nl

Keywords: $\mathcal{H}_\infty$, robust control, modeling, nonlinear dynamics.

Abstract

The development of an $\mathcal{H}_\infty$-controller for a mono-cycle is outlined. The controller design is based on an accurate model of a mono-cycle, derived in the paper, and it considers both performance and robustness specifications. To easily attain the specifications a two degree-of-freedom control scheme is investigated. The results are compared with those for a single degree-of-freedom $\mathcal{H}_\infty$ design and for a state-feedback controller based on pole placement techniques. The two $\mathcal{H}_\infty$ designs are shown to be a moderate improvement upon the state-feedback design. The differences between the one and two degree-of-freedom $\mathcal{H}_\infty$ design depend on the set of measured variables.

1. Introduction

The mono-cycle, a wheel and a frame with an actuated joint in between, is a motivating example for applications of modern control techniques. It is nonlinear, so control designs based on linearized models are not guaranteed to work well in practice, and its up-right position is unstable, so a controller is mandatory.

The longitudinal dynamics of a mono-cycle is comparable with that of the ubiquitous cart-pendulum system. The main difference between the systems is in the way they are actuated. A mono-cycle is slightly more involved, because here the torque that drives the wheel also directly influences the torque on the frame, even when the wheel is not moving, while for the inverted pendulum the force on the cart does not directly influence the pendulum, only the movement of the cart does.

The control of a mono-cycle has been studied previously, see [1–3]. The first paper considers a single-input/single-output (SISO) LQ(G) design for two control loops, the pitch and yaw loop, of a complete mono-cycle. For the yaw loop a nonlinear friction compensation term was added. Simulation and (limited) experimental results are provided. The other papers discuss a model that includes the human cyclist. They employ a human mimicking actuation setup (one could call this a robot driven mono-cycle) and show some simulation and experimental results. Another reference is [4]. Their approach is to use a sequential SISO loop shaping design, so multivariable $\mathcal{H}_\infty$ techniques are not employed. Also, although they claim to use a two degree-of-freedom control scheme, their implementation seems to use a single degree-of-freedom one, see [4, Fig. 3].

Controller design with an $\mathcal{H}_\infty$-norm criterion is well known, see, *e.g.*, [5, 6], and can be expressed in terms of Riccati equations [7]. The $\mathcal{H}_\infty$ approach can be used, as we will do, to express frequency domain specifications on several closed loop transfer functions.

The main goal of the paper, now, is to improve on the results in [4] and to present a worked example of an $\mathcal{H}_\infty$ controller design for a nonlinear mechanical system. The paper also provides an accurate model of a mono-cycle, gives detailed guidelines for its controller design, and discusses practical problems and solutions in the design of $\mathcal{H}_\infty$ controllers.

Section 2 presents a description and model of the mono-cycle. Section 3 details the control system specifications and the controller design. The evaluation of the controllers, in Section 4, and the ensuing discussion of the results, in Section 5, guides us in drawing conclusions and recommendations, related to the fulfillment of the main goal of the paper, in Section 6.

2. System description

The system considered is a mono-cycle, see Fig. 1. It consists of a wheel, a frame, and a motor with transmission. Additional guidance wheels, not shown in the figure, fix the position of the mono-cycle in the direction (the lateral direction) perpendicular to the direction of motion (the longitudinal direction). Eventually, these wheels may be replaced by a controlled reaction wheel. The control system, to be designed in this paper, only aims at stabilizing the frame in the up-right position in the plane of motion and at tracking a desired wheel axle position in the horizontal direction. The model of the system should at least describe the dynamic phenomena related to these tasks.

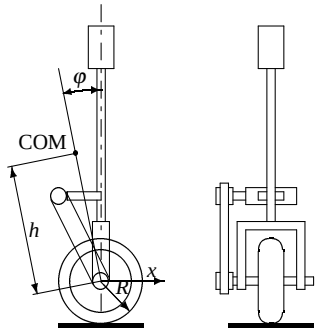

Figure 1: Mono-cycle

The equations of motion for mechanical systems can be derived with the Lagrange formalism, as is done in [4]. However, the equations in that paper are not correct. This forces us to give some details of our derivation and to justify our deviation from the model in [4].

Several formulations of Lagrange's equations are possible. In this paper the one is used where only the kinetic energy $E(\dot{q}, q)$ appears in the left hand side of the equation, as follows

$$\frac{\mathrm{d}}{\mathrm{d}t}\frac{\partial E}{\partial \dot{q}_j} - \frac{\partial E}{\partial q_j} = Q_j, \quad j = 1, \ldots, n. \tag{1}$$

Here, n is the number of degree-of-freedom's or generalized coordinates q and Q_j, $j = 1, \ldots, n$, are the generalized forces. They can be derived by the principle of virtual work.

Using as generalized coordinates q the horizontal displacement x of the center of the wheel and the angular rotation φ of the COM (center-of-mass) of the frame and motor (relative to the vertical and positive in clockwise direction), the kinetic energy of the wheel (with mass M_w, central moment of inertia J_w, and wheel radius R) is expressed as

$$E_w = \frac{1}{2}(M_w R^2 + J_w)\left(\frac{\dot{x}}{R}\right)^2$$

while the kinetic energy for the frame and motor rotor are

$$E_f = \frac{1}{2}\left\{M_f R^2\left(\left(\frac{\dot{x}}{R}\right)^2 + 2\frac{1}{R}\frac{\dot{x}}{R}\dot{\varphi}h\cos\varphi\right) + \left(M_f h^2 + J_f\right)\dot{\varphi}^2\right\}$$

$$E_m = \frac{1}{2}\frac{J_m}{i^2}\left(\frac{\dot{x}}{R} + (i-1)\dot{\varphi}\right)^2,$$

where M_f is the mass of the frame and the motor, J_f is the central moment of inertia around COM of the frame and the motor, except for the central moment of inertia J_m of the motor rotor, and h is the distance of the wheel axis to COM. Furthermore, i is the transmission ratio, such that $i\varphi_m = x/R - \varphi$, where φ_m is the rotation of the rotor with respect to its housing, *i.e.*, to the frame.

The virtual work δA for virtual changes of x and φ is

$$\delta A = \left\{ -\left(\frac{\nu}{i^2} + \mu\right)\left(\frac{\dot{x}}{R} - \dot{\varphi}\right) + \frac{\tau}{i} \right\}\left(\frac{\delta x}{R} - \delta\varphi\right) + M_f g h \sin\varphi \;\; \delta\varphi.$$

Here, τ is the motor torque, ν and μ are the coefficients of viscous damping in the bearings of the motor axis, respectively of the frame on the wheel axis, and g is the acceleration of gravity. Assuming the motor to be perfect, with no internal resistance nor back-EMF, we can write for the generated motor torque

$$\tau = au$$

with a the motor torque constant and u the control voltage. Now the generalized forces can be extracted from

$$\delta A = \delta q^T Q = \delta x Q_1 + \delta\varphi Q_2.$$

Using (1) with $E = E_w + E_f + E_m$ one gets equations of the form

$$M(q)\ddot{q} + C(\dot{q}, q)\dot{q} + G(\dot{q}, q) = H(q)u \tag{2}$$

with

$$M = \begin{bmatrix} M_w + M_f + \frac{1}{R^2}\left(J_w + \frac{1}{i^2}J_m\right) & M_f h\cos\varphi + \frac{1}{R}\frac{i-1}{i^2}J_m \\ M_f h\cos\varphi + \frac{1}{R}\frac{i-1}{i^2}J_m & M_f h^2 + J_f + \frac{(i-1)^2}{i^2}J_m \end{bmatrix}$$

$$C = \begin{bmatrix} 0 & -M_f\dot{\varphi}h\sin\varphi \\ 0 & 0 \end{bmatrix}$$

$$G = \begin{bmatrix} \frac{1}{R}\left(\frac{\nu}{i^2} + \mu\right)\left(\frac{\dot{x}}{R} - \dot{\varphi}\right) \\ -M_f g h\sin\varphi + \left(\frac{\nu}{i^2} + \mu\right)\left(\dot{\varphi} - \frac{\dot{x}}{R}\right) \end{bmatrix}$$

$$H = \frac{a}{i}\begin{bmatrix} \frac{1}{R} \\ -1 \end{bmatrix}.$$

There are several differences with the equations of motion given in [4]. The first is in the right hand side of (2) where they have $H_2 = 0$ instead of $H_2 = -a/i$, the second is the term $-M_f\dot{\varphi}^2 h\sin\varphi$ in the first equation while they have a Coriolis term containing $\dot{x}\dot{\varphi}$ in the second equation, the third is in the way the viscous friction terms are handled. The last difference is due to the incorporation of the motor rotor inertia J_m and the introduction of the transmission ratio i. Another model, with a larger number of degree-of-freedom's, is presented in [1]. In addition to the longitudinal dynamics of [1], our model includes the inertia and viscous friction of the motor and the viscous friction for the relative motion of wheel and frame. Furthermore, in their model only the nonlinear terms in which yaw rate or yaw acceleration appear are considered, the other terms are linearized. This means that the term with $\dot{\varphi}^2$ in the first equation of (2) is neglected, also the goniometric terms are linearized, so for the frame angle the sin-terms are replaced by the angle and the cos-terms are replaced by 1. Finally, their model only includes the wheel rotational speed as component of the state and output, while we use the wheel position, because we will consider a tracking problem for the position of the mono-cycle. We conclude that our longitudinal dynamics model improves on the two other models considered and is suitable for tracking control.

Linearizing (2) around $\varphi = 0$ with the parameters in Table 1 gives

$$\dot{z} = \begin{bmatrix} 0 & 0 & 1 & 0 \\ 0 & 0 & 0 & 1 \\ 0 & -3.6169 & -22.7377 & 4.5475 \\ 0 & 20.9311 & 58.2953 & -11.6591 \end{bmatrix} z + \begin{bmatrix} 0 \\ 0 \\ 5.6089 \\ -14.3802 \end{bmatrix} u$$

where the state z is defined by

$$z = \begin{bmatrix} q_1 & q_2 & \dot{q}_1 & \dot{q}_2 \end{bmatrix}^T = \begin{bmatrix} x & \varphi & \dot{x} & \dot{\varphi} \end{bmatrix}^T.$$

To get results comparable to the results in [4] the parameters J_m and i are given values such that they have no influence on the dynamics. The system is unstable, as could be expected. This is also clear from inspecting the system matrix: at least one pole is in the RHP (right-half-plane) and one pole is at the origin.

Table 1: Model parameters. The first set is taken from [4]

Parameter	Description	Value	Unit
M_w	wheel mass	1.5	kg
M_f	frame and motor mass	6.0	kg
J_w	wheel inertia	0.2	kg m^2
J_f	frame inertia	0.608	kg m^2
R	wheel radius	0.2	m
h	distance COM to wheel axis	0.36	m
ν	motor rotor friction	6.33	Nms/rad
μ	wheel bearing friction	2.12	mNms/rad
a	motor torque constant	7.81	Nm/V
J_m	motor rotor inertia	0.	kg m^2
i	transmission ratio	1.	-
g	acceleration of gravity	9.81	m/s^2

The transfer function matrix corresponding with the state space model, using u as input and $\left[\begin{smallmatrix} x \\ \varphi \end{smallmatrix}\right]$ as output, is

$$P_n = \begin{bmatrix} \frac{5.6089s^2 - 65.3886}{s^4 + 34.3967s^3 - 20.9311s^2 - 265.0760s} \\ \frac{-14.3802s^2}{s^4 + 34.3967s^3 - 20.9311s^2 - 265.0760s} \end{bmatrix}.$$

It is easy to see that with φ alone the system will not be observable since a pole and zero at the origin will cancel in P_n. The output x will be sufficient for observability. The transfer function from u to x is nonminimum phase, a property that should be carried over to the closed loop system, and from u to φ there are zeros at the origin. The corresponding transfer function derived in [4] is equal to (after some corrections to the data used there)

$$P_o = \begin{bmatrix} \frac{0.247}{s(1 + .079s)} \\ \frac{-10.15}{s^2 + .43\cdot 10^{-3}s - 15.29} \end{bmatrix}$$

with each individual transfer function of lower order than in P_n due to additional (ad-hoc) simplifications. The difference between the two models is illustrated in Figs. 2–3 presenting the transfer function amplitudes.

3. Controller design

Three controllers were designed: two $\mathcal{H}_\infty$ controllers, respectively for a control system with one and two degree-of-freedom, and one state-feedback controller

An analysis of the system matrix of the linearized model shows that the system is unstable, with one pole in the RHP and one on the imaginary axis. The state-feedback controller was designed with pole placement techniques by reflecting the unstable pole to the left-half-plane and then shifting all four poles by –1. This resulted in the state-feedback controller

$$u = -K^{sf} z$$

with

$$K^{sf} = \begin{bmatrix} -7.7461 & -27.2204 & -16.1393 & -6.9847 \end{bmatrix}$$

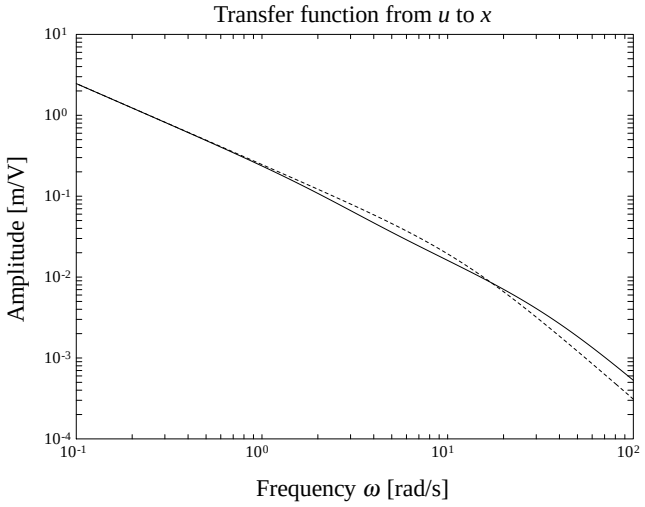

Figure 2: Comparison of models. –: P_n, - -: P_o

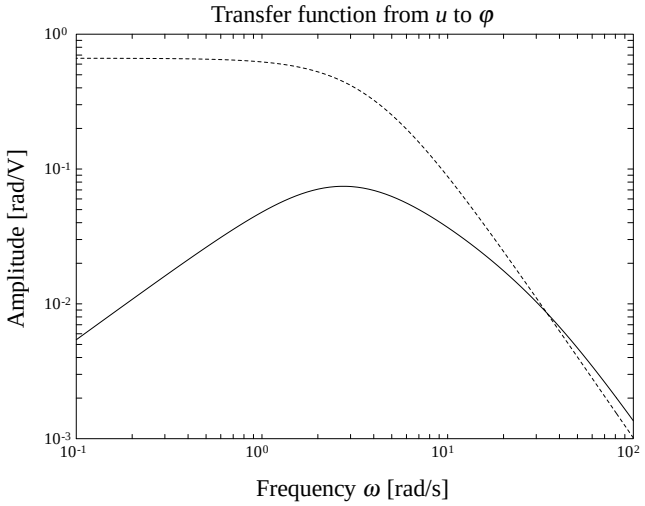

Figure 3: Comparison of models. –: P_n, - -: P_o

that realized the following closed loop poles

$$-1.0000 \quad -3.5760 \quad -3.9587 \quad -35.7794.$$

This control law is suitable for regulation, but not for tracking. The controller was therefore modified to

$$u = \begin{bmatrix} K_1^{\mathrm{sf}} & -K^{\mathrm{sf}} \end{bmatrix} \begin{bmatrix} r \\ z \end{bmatrix}$$

where r is the desired value for the position x and K_1^{sf} is the first component of K^{sf}. With this tracking control law all state-feedback results are obtained.

The design of the $\mathcal{H}_\infty$ controllers is based mainly on the same criteria as used in [4], but with a completely different design procedure. The design in [4] is sequential with two nested SISO designs. The design procedure and specifications we use circumvent the problem mentioned in [4] that their controller was only stabilizing but could not track a reference signal for x without additional modifications. Our design results in a controller that does not only stabilize the system, but is also able to track a reference signal for x, within the restrictions placed by the physics of the system and by the fact that the design is based on the linearized model. The physical restrictions imply that the closed loop system should show an initial inverse response for a required step-wise change in x, and the use of the linearized model implies that the results are only valid locally.

The strategy used is to translate the specifications on the controlled system to a mixed sensitivity criterion, where the $\mathcal{H}_\infty$-norm based design is used to approximately shape several sensitivity and complementary sensitivity functions of the closed loop plant, because those transfer functions are closely related to the specifications.

For the specification some additional input signals are introduced, namely the disturbances d_x and d_φ and the reference position r, leading to the disturbed outputs $x_d = x + d_x$, $\varphi_d = \varphi + d_\varphi$ and the tracking error $e = r - x_d$. The disturbances account for model errors. The additional inputs are incorporated in an extended plant P_e, together with some performance related outputs, see Fig. 4.

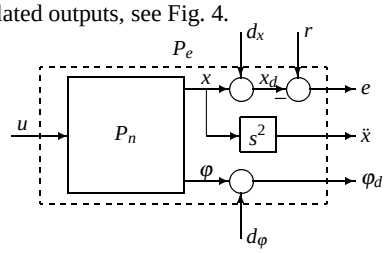

Figure 4: Extended plant

The desired bound for the complementary sensitivity function $T_{x_d r}$, from the reference r to the disturbed position x_d, is a double integrator, see [4], and is related to robustness for high-frequency unmodeled dynamics, so it aims at getting $T_{x_d r}$ small for high frequencies. For low frequencies there are no direct demands on $T_{x_d r}$, but there are on S_{er}, see later, so indirectly on $T_{x_d r}$ because $T_{x_d r} + S_{er} = 1$. The corresponding weight is a double differentiator, so we require

$$|T_{x_d r} \rho s^2|_\infty < 1$$

with ρ a tuning parameter. If one composes the weight and plant model P_n using state space models, this poses a problem because ρs^2 is not realizable in this form. This can be solved by using a state tapping technique [8]. For this an additional output of the plant is defined, namely the acceleration $\ddot{x}$. This signal can be used to achieve the design goal for $T_{x_d r}$ by requiring

$$|T_{\ddot{x} r} \rho|_\infty < 1.$$

The sensitivity function $S_{\varphi_d d_\varphi}$, for the transfer of the output disturbance d_φ to the disturbed angle φ_d, should be small for low frequencies to attenuate the effects of disturbances and to guarantee robustness for certain types of model errors. The inverse of its desired bound is specified in [4] by the biproper weight

$$\frac{(0.14s + 1)^2}{(0.24s)^2}.$$

However, for our model the transfer function $S_{\varphi_d d_\varphi}$ is "fixed" or "invariant", in the sense that its low frequency amplitude is equal to 1, irrespective of the controller used. A system theoretic interpretation of the origin of the restriction is in terms of interpolation constraints on (complementary) sensitivity functions if the plant has poles or zeros in the closed RHP. Here the transfer function from u to φ has zeros on the imaginary axis. The constraint implies that the previous weight makes no sense, it forces $|S_{\varphi_d d_\varphi}|$ to 0 for low frequencies and this is not feasible. To solve this conflict we choose a constant weight for the sensitivity function that does not violate the restriction.

Besides the two previous goals, an additional one is the tracking performance for the reference position r. For this the sensitivity function S_{er} between r and the tracking error e should be shaped. Ideally this would be small for all frequencies, but this is not possible due to the $T_{x_d r}$ specification. Therefore the following considerations are used. A steady state error of the order of $10^{-3} r$ [m] and sensitivity smaller than 1 for frequencies up to ≈1 [rad/s] are desired. This leads to the

specification

$$\left| S_{er} \frac{\alpha s + 1}{s + 0.001} \right|_\infty < 1, \quad \alpha \ll 1.$$

The value for α should not be taken too small for reasons mentioned below. It should also not be too large, like ρ, to make the bounds on $T_{x_d r}$ and S_{er} compatible.

A last goal is a limited torque exerted by the motor. Because the transfer function $T_{x_d r}$ implicitly limits the input u and not to make the design unduly involved, no additional weight was introduced for u.

To assure the adequacy of the controllers, to test their robustness, and to aid in the selection of design parameters α, ρ, and V, the evaluation of the performance will be established with a simulation using the full nonlinear model (2). So, we do not restrict ourselves to an evaluation of the design with the linear model. In the time domain evaluation we strive for the following objectives: a rise time of ≈4 [s], preferably no overshoot, and limited excursion of the angle φ, all for the responses on a step change in r. The angle φ should be limited to avoid large differences between the linear and nonlinear model, and so to keep the model errors small. The maximal input voltage to the motor is assumed to be 10 [V]. Because the system should function well in a time domain setting, the time domain specifications have preference above the frequency domain ones. This implies that the tuning of the frequency domain bounds and weights is guided by time domain evaluation results.

To facilitate the design, use is made of the MHC (Multivariable $\mathcal{H}_\infty$ Design) toolbox, see [9]. The setup of the design should therefore be brought in the standard form of Fig. 5, with G the generalized plant and K the controller. Ideally, what we would like the controller to achieve is the three specification simultaneously and nothing more than that. This can be achieved only approximately if using the standard setup.

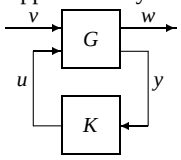

Figure 5: Standard design setup

To form the generalized plant G, the three weighting functions discussed above are all placed at the appropriate outputs of the extended plant, namely e, $\ddot{x}$, and φ_d, and are combined in a single diagonal transfer function matrix W. In addition, a constant diagonal input weighting matrix V is introduced that scales the three inputs, namely r, d_x, and d_φ, relevant for the specifications. The extended plant P_e and the weights V and W are combined to get the generalized plant G, see Fig. 6, where only the performance variables are detailed, but not the controller input y and output u.

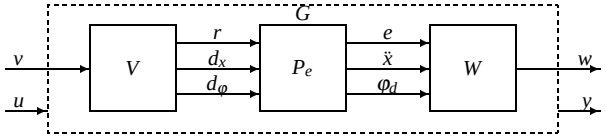

Figure 6: Generalized plant

Now the $\mathcal{H}_\infty$ design is performed by trying to arrive at a stabilizing controller $K(s)$ that achieves the following objective

$$\|F_l(G(s), K(s))\|_\infty < 1$$

with $F_l(\cdot)$ the lower fractional transformation, for the largest possible ρ and for suitable choices for the scaling parameters in V, where $F_l(G, K)$ is the transfer function matrix of the generalized closed loop plant from v to w. This setup ensures that the specifications are met (if such a $K(s)$ exists), but is hindered by the fact that also other transfer functions, for which no targets are set, are shaped. It is possible that those other transfer functions, *e.g.*, from v_1 to w_3, will contribute heavily to the $\mathcal{H}_\infty$-norm. This has to be checked and may eventually lead to an adaptation of the weight functions, possibly leading to non-diagonal weights.

For the $\mathcal{H}_\infty$ controller we use two schemes, resulting in a one and a two degree-of-freedom controller. This is illustrated in Fig. 7. Remark that for both controller schemes additional signals are needed to form the correct y. This only leads to a trivial modification of the extended plant, that we do not detail here.

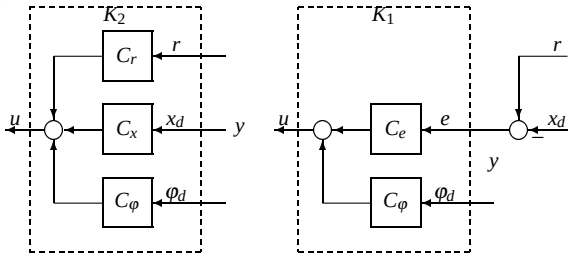

Figure 7: Control schemes. Left: two, right: one degree-of-freedom

The actual computation of the controllers with MHC and the software described in [10], was relatively straightforward and posed no interesting problems that are worth a further elaboration. We only make some remarks that are related to the existence conditions for the algorithm employed for the $\mathcal{H}_\infty$ design. First, it was necessary to regularize the plant model to shift the poles away from the imaginary axis. This was achieved by giving the (3,1) entry of the system matrix the value 10^{-3} instead of 0, shifting all poles by less than 10^{-3}. Secondly, the constant scaling in V for the disturbance d_x can be chosen 0 for the one degree-of-freedom design, but should be nonzero for the two degree-of-freedom design, to satisfy the rank condition for the block partition G_{21} of the generalized plant at infinity. This partition relates v to y. In both designs the scaling was set at the same value, so not to let the specifications depend on the control scheme.

The tuning of the remaining parameters in the weights V and W, necessary to arrive at an acceptable time domain performance, is a bit cumbersome, but using trial and error with an interactive tool like MHC it is not too time consuming when time is not spent by just fiddling with the weighting function parameters, but with a well thought out approach using incremental weight changes and based on inspection of the frequency and time domain performance measure details.

As stated before, the value for α should not be taken too small, for then the controller may contain a very fast pole at $-1/\alpha$ (this depends on the design, *e.g.*, the choice of weighting functions). This makes the controller difficult to discretize with reasonable sampling times (this is only relevant for a discrete time implementation of the controller which we do not consider here) and increases the simulation time. A suitable compromise is $\alpha = 0.05$. Another factor that determines the poles of the controller is the distance of the achieved $\mathcal{H}_\infty$-norm to the exact optimum. By slightly backing of the design, the faster controller pole does not move quite so far to the left in the complex plane as would happen nearer to the optimum.

For the final choice of parameters and weight functions we ended up with the following scalings V and weight functions W

$$V = \begin{bmatrix} \frac{2}{3} & 0 & 0 \\ 0 & \frac{1}{100} & 0 \\ 0 & 0 & \frac{2}{100} \end{bmatrix} \quad W = \begin{bmatrix} \dfrac{.05s + 1}{s + .001} & 0 & 0 \\ 0 & \rho & 0 \\ 0 & 0 & \frac{1}{4} \end{bmatrix}.$$

For the one degree-of-freedom design we could achieve a value for ρ of 0.6, and for the two degree-of-freedom a ρ of 0.6 also, giving an $\mathcal{H}_\infty$-norm slightly larger than 1, namely 1.03. Contrary to what could be expected, the additional design freedom makes it hardly possible to improve the robustness specifications of the system. This could be inferred from the transfer function matrix of the two degree-of-freedom controller, in which the transfer function amplitudes from r to u and from x_d to u are often almost indistinguishable. When using only a single measurement, namely x_d, there is a significant difference between controllers using e only, or using both r and x_d. The two degree-of-freedom scheme uses the additional design freedom effectively with the restricted measurements, and performs much better

than the one degree-of-freedom one. So for this case a two degree-of-freedom scheme is better. We remark also that, although the closed loop was stable, both $\mathcal{H}_\infty$ controllers were unstable. This is not always desirable in practice.

4. Results

The evaluation of the frequency domain design objectives is done with the linearized model, but the time domain evaluation of the design, for robustness and usability, uses the nonlinear model.

First, we present the results with the state-feedback controller, and use this to compare results with the linearized and the nonlinear model. Step responses for both outputs and both models are in Figs. 8–9.

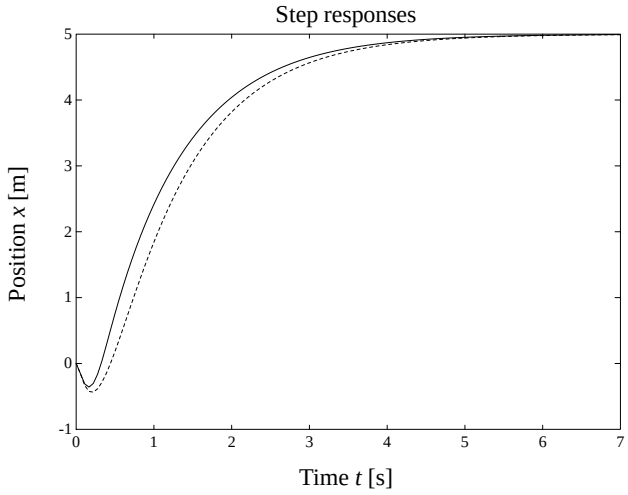

Figure 8: Step response for x, state-feedback. –: nonlinear model, - -: linearized model

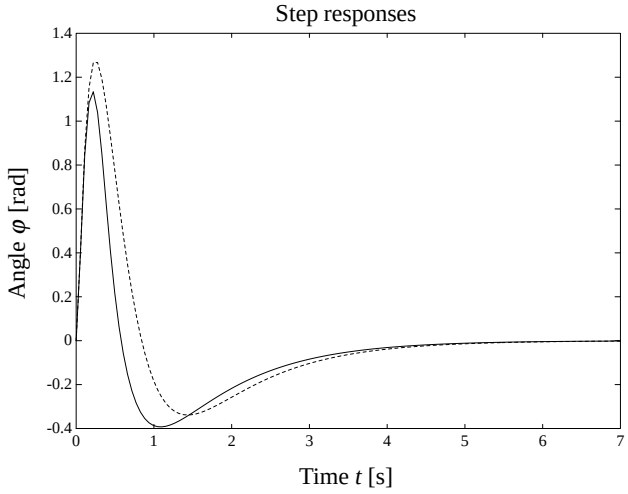

Figure 9: Step response for φ, state-feedback. –: nonlinear model, - -: linearized model

Remark that only with large step amplitudes for r the differences between linearized and nonlinear model are significant. The value we used, $r = 5$ [m], is already quite extreme and unlikely to occur in practice. Nevertheless, the differences are moderate. If still larger steps are asked for, *e.g.*, $r = 10$ [m], the closed loop nonlinear model leaves the domain of attraction of the upright equilibrium point. For some values of r in between the ones mentioned above, it is possible for the controller to position the wheel, but the frame may complete a full turn before it stabilizes in the up-right position. This is possible in the simulation, but not in practice. For a step of 5 [m] the input u is slightly larger than its bound.

Secondly, we evaluate the $\mathcal{H}_\infty$ controllers in the frequency domain. Figures 10–11 show the main transfer functions of the closed loop system, excluding the weights V and W, in comparison with the bounds.

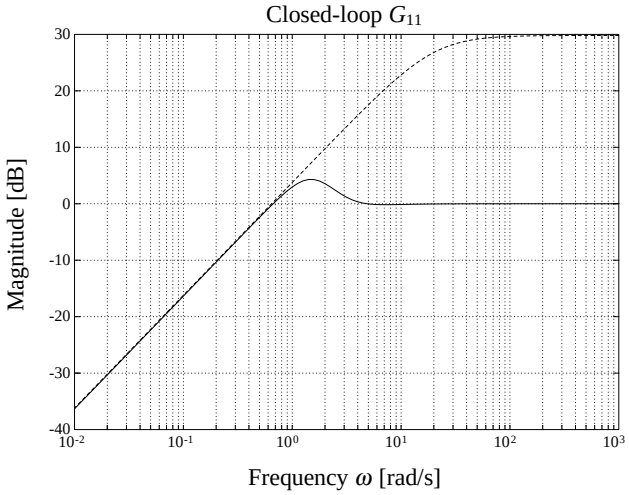

Figure 10: Transfer function from r to e, –, and bound, - -

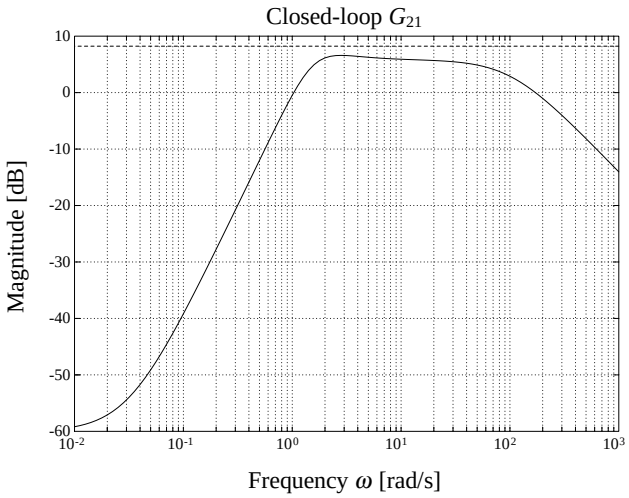

Figure 11: Transfer function from r to $\ddot{x}$, –, and bound, - -

It is apparent that the design goals are not completely achieved. Although the $\mathcal{H}_\infty$-norm of the generalized closed loop plant was very close to 1, namely 1.03, the scaling of v_1, thus r, by 2/3 shows that the objective for S_{er} is achieved modulo this factor only. It is possible to set the scaling for v_1 to 1 and reduce the factor ρ, and by that achieve the goal for S_{er}, but then the rise time was faster then required and the maximum frame angle φ was significantly larger during a step response. This indicated a situation with a smaller region of stable operation of the closed loop, that was not deemed acceptable, motivating the choice for a scaling by 2/3.

Finally, the performance of the $\mathcal{H}_\infty$ controllers in the time domain is evaluated. Figures 12–13 show time responses for a desired step change in the position x, again of 5 [m]. For all three controllers the nonlinear model is used.

It is clear from these results that the controllers are able to achieve the tracking goal, but the two $\mathcal{H}_\infty$ controllers provide for a better tracking behavior: the desired wheel axle position, r, is reached slightly faster, without increasing the maximum frame angle, φ. In general, the $\mathcal{H}_\infty$ controllers were able to stabilize the system for larger excursions from the equilibrium position. For both $\mathcal{H}_\infty$ controllers the input u was within its bound of 10 [V] for steps smaller than 5 [m]. For larger steps the bound may be violated. Remark that the responses for the two $\mathcal{H}_\infty$ controllers are almost indistinguishable from each other and that they exhibit a slight overshoot.

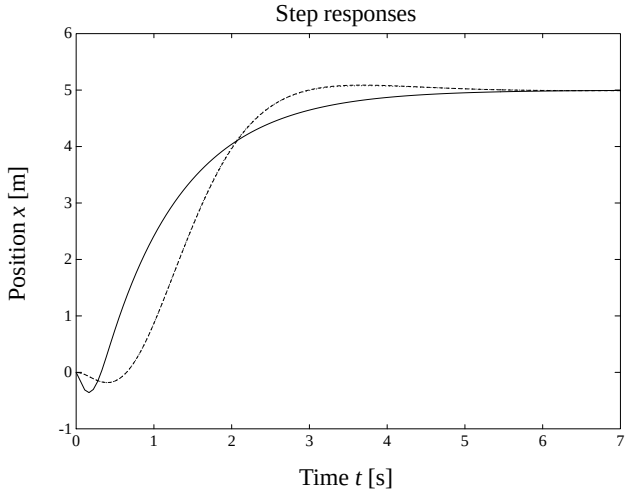

Figure 12: Time responses. –: State feedback, - -: $\mathcal{H}_\infty$ with one degree-of-freedom, $\cdots$: $\mathcal{H}_\infty$ with two degree-of-freedom

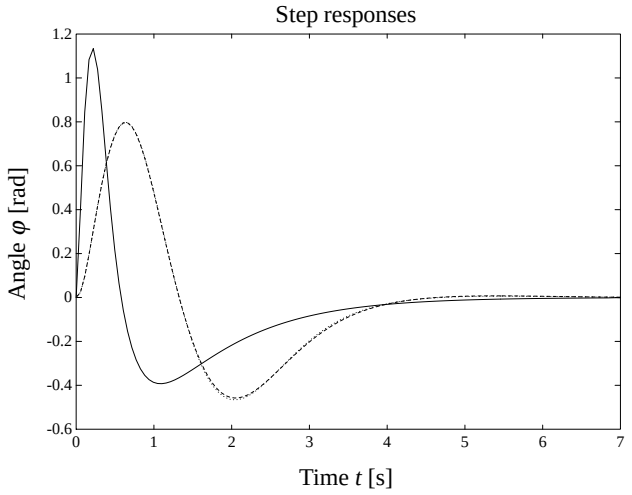

Figure 13: Time responses. –: State feedback, - -: $\mathcal{H}_\infty$ with one degree-of-freedom, $\cdots$: $\mathcal{H}_\infty$ with two degree-of-freedom

5. Discussion

All three designs perform acceptable. The state-feedback controller excels in having no overshoot, but is more sluggish and gives larger values for the frame angle φ. We did not try to optimize the pole locations of the closed loop, so a better state-feedback controller is imaginable. The $\mathcal{H}_\infty$ designs perform slightly better for both the tracking error, with a smaller rise time, and the frame angle, with a smaller maximum value, but have some overshoot. Furthermore, they only need position and frame angle measurements, but are dynamic controllers and unstable. The state-feedback controller needs measurements of all states, that will be difficult or expensive in practice, but is a static controller and therefore its stability is not an issue. The controlled systems were also quite robust, for differences between the nonlinear and linearized model, and able to withstand significant deviations from the up-right position. Especially the $\mathcal{H}_\infty$ controllers did well with respect to this point.

It may be possible for other control structures to be better suited for mono-cycle control. A first option is to improve the mixed sensitivity design by using a μ-synthesis approach, with two blocks, one related to r and one to d_φ, instead of a straight $\mathcal{H}_\infty$ design. With two blocks it is possible to reduce some conservatism in the design. One may also think of nonlinear controllers, *e.g.*, nonlinear $\mathcal{H}_\infty$ controllers, with a larger stability region or better tracking performance, or of adaptive controllers that would not require accurate model parameters to function well. Examples of nonlinear $\mathcal{H}_\infty$ controllers, in this case applied to a 2-DOF robot and a cart-pendulum model, respectively, are provided in [11,12]. The first reference discusses a nonlinear $\mathcal{H}_\infty$ design directly targeted at the specific class of models for robotic systems. The second reference shows that a nonlinear $\mathcal{H}_\infty$ controller is able to cope with larger disturbances before leaving the area of the state space for which the equilibrium point is attractive, compared with its linear $\mathcal{H}_\infty$ control equivalent. The feasibility of these and other control schemes for the mono-cycle should be verified.

6. Conclusions and Recommendation

In this paper an enhanced model for a mono-cycle has been derived. Based on a linearized model three controllers are designed to stabilize the system and to allow tracking of a desired position. The design set-up was quite flexible with ample provisions for tuning, but with appropriate interactive tools like MHC this was not too time consuming. All controllers performed acceptable and did not show the problems with tracking a desired wheel axis position as reported previously. The controllers are also quite robust, *i.e.*, they performed well with the nonlinear model for a large range of the state variables, not only close to the nominal equilibrium point. For the set of measurements employed, the two degree-of-freedom scheme showed no advantages. With limited instrumentation, only measuring the position x, the one degree-of-freedom scheme showed some weaknesses.

It appears possible to use the mono-cycle for a design project. Carrying out this project enables an experimental evaluation of the control schemes. The practical feasibility of the current and other control schemes can then be verified.

References

[1] D. W. Vos and A. H. von Flotow, "Dynamics and nonlinear adaptive control of an autonomous unicycle: Theory and experiment," in *Proc. of the 29th IEEE Conf. on Decision and Control*, vol. 1, (Honolulu, Hawaii), pp. 182–187, IEEE, Dec. 1990.

[2] Z. Sheng and K. Yamafuji, "Study on the stability and motion control of a unicycle, (Part I: Dynamics of a human riding a unicycle and its modeling by link mechanisms)," *JSME Internat. J., Series C*, vol. 38, pp. 249–259, June 1995.

[3] Z. Sheng, K. Yamafuji, and S. V. Ulyanov, "Study on the stability and motion control of a unicycle, (3rd Report, Characteristics of a unicycle robot)," *JSME Internat. J., Series C*, vol. 39, pp. 560–568, Sept. 1996.

[4] F. Takemori and Y. Okuyama, "Stabilizing control of a mono-cycle based on H_∞ control theory — Detection of the attitude by using a visual sensor —," in *Proc. of the Asian Control Conf.*, vol. 1, (Tokyo, Japan), pp. 591–595, July 1994.

[5] J. M. Maciejowski, *Multivariable Feedback Design*. Wokingham: Addison-Wesley, 1989.

[6] B. A. Francis, *A Course in H_∞ Control Theory*. Berlin: Springer-Verlag, 1987.

[7] J. C. Doyle, K. Glover, P. P. Khargonekar, and B. A. Francis, "State-space solutions to standard H_2 and H_∞ control problems," *IEEE Trans. Automat. Control*, vol. AC–34, pp. 831–847, Aug. 1989.

[8] J. M. Krause, "Comments on Grimble's comments on Stein's comments on rolloff of H^∞ optimal controllers," *IEEE Trans. Automat. Control*, vol. 37, p. 702, May 1992.

[9] H. M. Falkus, "H_∞ robust control design for an electromechanical servo system," in *Proc. of the first European Control Conf.*, vol. 3, (Grenoble, France), pp. 2478–2483, Paris: Hermès, July 1991.

[10] R. Y. Chiang and M. G. Safonov, *Robust Control Toolbox User's Guide*. Natick, MA: The MathWorks, Inc., Aug. 1992.

[11] D. de Vries, "Design of a nonlinear H_∞ controller for a 2-DOF robot," MSc thesis, Dept. of Applied Mathematics, University of Twente, Enschede, The Netherlands, Nov. 1994.

[12] J. Møller-Pedersen and M. P. Petersen, "Control of nonlinear plants – Volumes I and II," MSc thesis, Mathematical Institute, Technical University of Denmark, Lyngby, Denmark, Aug. 1995.